Supplementary Information

(Dated: March 25, 2023)

Appendix A: Bands and density of states for PT slabs

This section contains plots of the bands and density of states (DOS) for a (single) Pöschl-Teller (PT) slab. It relates the qualitative behavior of the kinetic energy to the behavior of the DOS within various AE approximations.

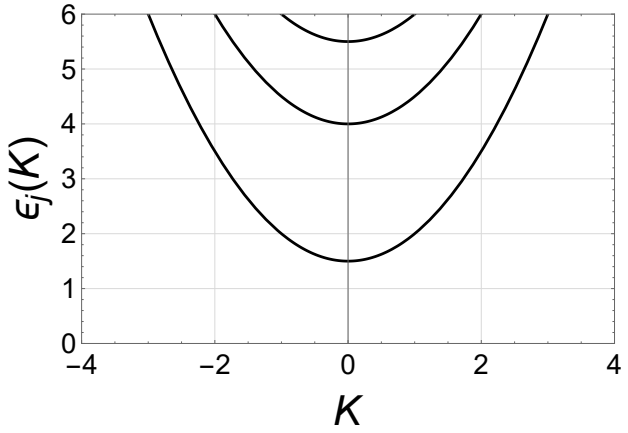

FIG. S1. The eigenvalues of the, $D = 6$, PT slab as a function of the parallel wave vector K.

Figure S1 shows the simple shape of the PT slab bands, which are free-electron like in the two directions perpendicular to $v(x)$ and begin at each of the eigenvalues of the 1D well. The system is a band metal.

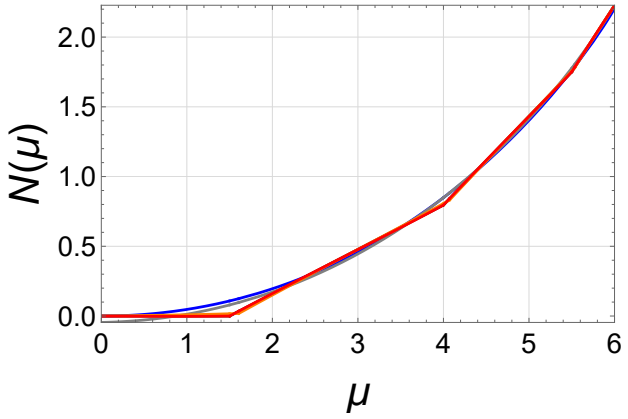

FIG. S2. The, $D = 6$, PT slab occupation (black), and its TF (blue), GEA2 (gray), AEA2' (orange), and AEA2 (red) approximations.

Figure S2 shows the number staircase (integrated DOS) for a given PT slab. The function is rather smooth, making it difficult to see differences between approximations. However, there are kinks in the exact curve whenever a new band begins to be occupied. Both the TF and GEA2 curves have no such kinks. Although TF is often considered to give 'the' smooth curve, there is a small but finite correction from the second order GEA.

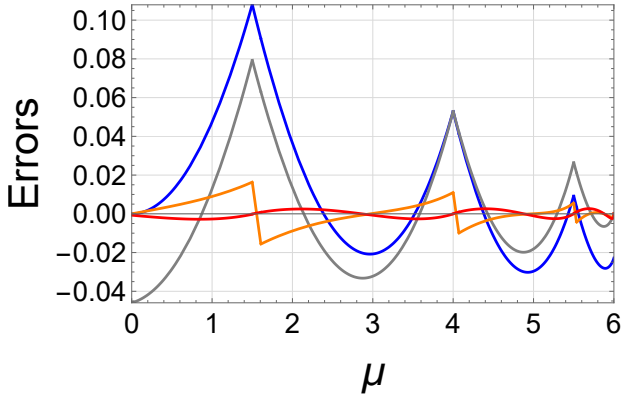

FIG. S3. The errors in Fig. S2.

Figure S3 plots the errors (defined as approximate minus exact) in the number staircase of the various approximations. The TF and GEA2 error curves have kinks because they are smooth, but the exact curve is not. The orange curve is AEA2', which only accounts for the leading behavior of the phase, while the red curve is AEA2, which includes the next contribution to the phase. Their difference becomes negligible for sufficiently large μ (both are asymptotically correct), but AEA2 clearly has smaller errors for small μ.

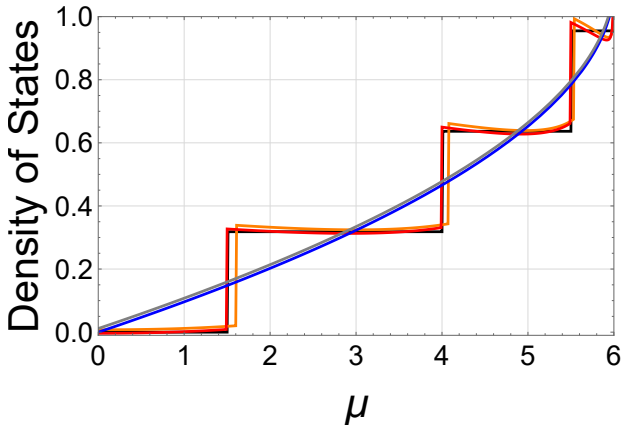

FIG. S4. The, $D = 6$, PT slab density of states $dN/d\mu$ (black), and its TF (blue), GEA2 (gray), AEA2' (orange), and AEA2 (red) approximations.

Figure S4 shows the density of states of a particular PT slab. This is just the derivative of the number staircase given in Eq. (1) of the main text and shown in Fig. S2. Both TF and GEA2 yield smooth approximations to it, and miss the discrete steps (the origin of

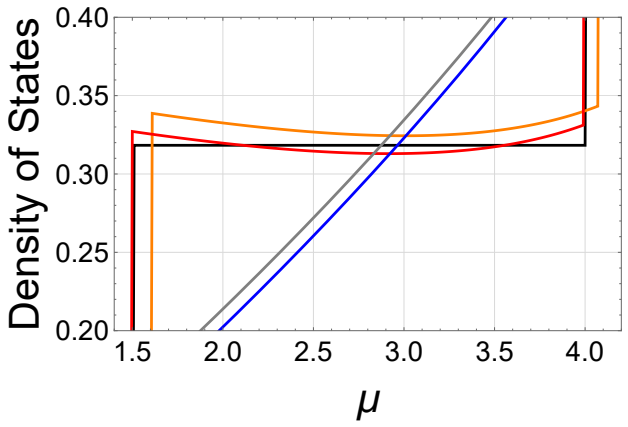

FIG. S5. A zoomed in view of Fig. S4.

the infamous DFT derivative discontinuity [54]). Unlike how it is treated in many semiclassical works [29], the smooth curve is not synonymous with the TF contribution, as GEA2 makes a small but finite correction. The asymptotic expansion approximation contains approximate steps, with approximations to the plateau in between. The exact DOS jumps discontinuously when $\mu = \epsilon_j$ where the ϵ_j are the exact 1D eigenvalues. Using the definition of the saw-tooth function $\langle x \rangle = x - \lfloor x + 1/2 \rfloor$ we can show that the AEA2' approximation jumps when

$$s^{(0)}(\mu) = j + \frac{1}{2}, \qquad j = 0, 1, 2, \cdots . \tag{A1}$$

This is just the lowest order WKB quantization rule for a single 1D well [55]. This means that AEA2' jumps when $\mu = \epsilon_j^{(0)}$, the jth WKB eigenvalue. Similar analysis shows that AEA2 jumps when

$$s^{(2)}(\mu) = j + \frac{1}{2}, \qquad j = 0, 1, 2, \cdots , \tag{A2}$$

which is just the second order WKB quantization rule from Eq. (2) of the main text. Thus AEA2 jumps when $\mu = \epsilon_j^{(2)}$, the second order WKB eigenvalue. AEA2 is much more accurate, as Fig. S5 shows, because $\epsilon_j^{(2)}$ is a better approximation to ϵ_j than $\epsilon_j^{(0)}$. The inaccuracies in both second order AEAs vanish as μ becomes large. Neither curve is quite flat, but AEA2 is flatter than AEA2'.

Appendix B: Densities and potentials

This section contains PT slab densities and PT dimer potentials. Figure S6 shows exact densities, from Table I of the main text, and their TF approximation–we scaled the densities so that the TF density is the same for all values of M. As M increases we approach the semiclassical limit and these densities weakly approach their TF counterpart. Because the chemical potential (relative to well-depth) is held fixed but the particle number is not

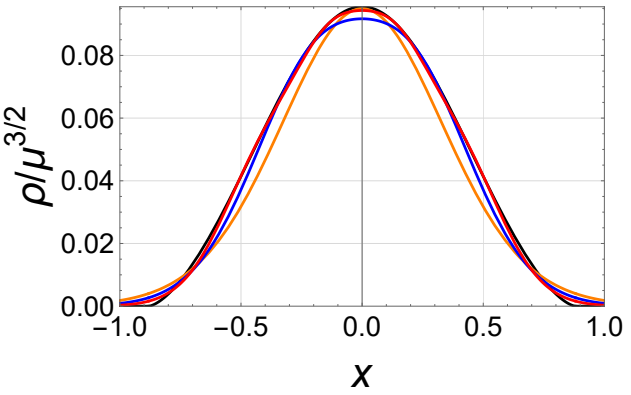

FIG. S6. Densities for $M = 1$ (orange), 2 (blue), 4 (red), and their TF limiting value (black). The areas under the curves are TF (0.0879), M = 1 (0.0809), M = 2 (0.0854), M = 4 (0.0871).

(unlike in Fig. 2 of Ref. [44]), the normalization changes, but approaches that of TF in the limit.

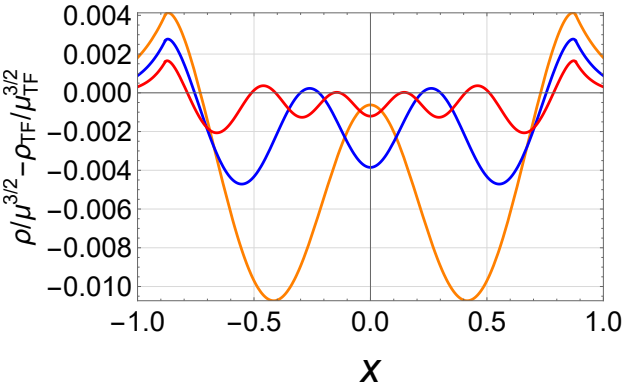

FIG. S7. The deviation of the exact scaled densities in Fig. S6 from the scaled TF density. The exact chemical potential is μ and $\mu_{\rm TF}$ is its TF approximation.

Figure S7 simply shows the differences from the TF curve in Fig. S6, making the weak approach to zero evident. Here, weak means that the integral over any well-behaved function times the density approaches its TF counterpart [56].

Figure S8 shows the various potentials of the PT dimer slabs as a function of their separation, given in units of the critical separation at which the second derivative of the midpoint potential vanishes. Beyond this critical value, there are two wells, and the form of the semiclassical asymptotic expansion presented in this work fails.

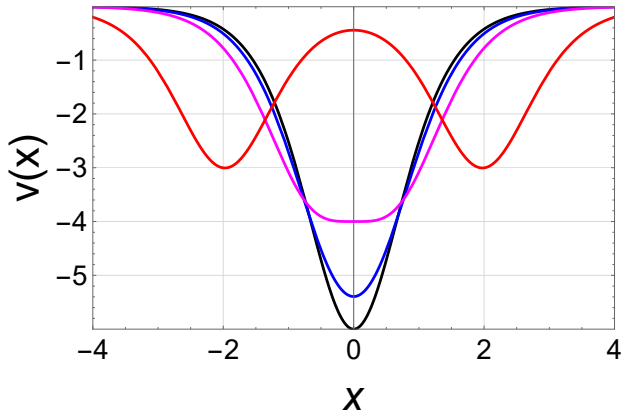

FIG. S8. Several PT dimer potentials made from 2, $D = 3$, PT slabs at various separations: $R/R_c = 0$, 0.5, 1, 3 (black, blue, magenta, red), $R_c = 2\,\mathrm{asech}\sqrt{2/3} = 1.31696$.

Appendix C: Expansion of the 1D action and the derivation and numerical calculation of AEA approximations

The number staircase for the 1D potential $v(x)$ is

$$n(\mu) = \sum_{j=0}^{\infty} \Theta(\mu - \epsilon_j), \tag{C1}$$

where $\Theta(x)$ is the Heaviside step function. It counts the number of occupied levels in a 1D well for a given μ. It can also be written as [24]

$$n(\mu) = s(\mu) - \langle s(\mu) \rangle\,. \tag{C2}$$

This form is more useful for deriving semiclassical approximations to $n(\mu)$ order by order. To derive such approximations we need to expand $s(\mu)$. To fourth order the expansion of the action is [37]

$$\begin{aligned} s^{(0)}(\mu) &= \int dx\, \frac{p_{\rm F}(x)}{\pi}, \qquad \Delta s^{(2)}(\mu) = -\frac{I''(\mu)}{3}, \\ \Delta s^{(4)}(\mu) &= \frac{J'''(\mu)}{5760}, \end{aligned} \tag{C3}$$

where I is in the main text and

$$J = \int dx \frac{7v''(x)^2 - 5v^{(4)}(x)p_{\rm F}(x)^2}{\pi\, p_{\rm F}(x)}, \tag{C4}$$

where again all integration is between the two classical turning points and $v^{(n)}(x)$ is the n-th derivative of $v(x)$.

We define two M-th order 1D number staircase expansions

$$\begin{aligned} n^{(M')}(\mu) &= s^{(M)}(\mu) - \left\langle s^{(M-2)}(\mu) \right\rangle, \\ n^{(M)}(\mu) &= s^{(M)}(\mu) - \left\langle s^{(M)}(\mu) \right\rangle, \end{aligned} \tag{C5}$$

and $n^{(0')}(\mu) = s^{(0)}(\mu)$.

The slab particle number is related to the 1D number staircase via

$$N(\mu) = \int_0^{\mu} d\epsilon\, \frac{n(\epsilon)}{\pi}. \tag{C6}$$

Plugging in $n^{(2)}$ ($n^{(2')}$) and collecting the second order terms yields the AEA2(2') approximation to N.

In this paper we calculate $N^{\rm AEA4'}(\mu)$, the AEA4' approximation to $N(\mu)$, numerically. We start by plugging $n^{(4')}$ into Eq.(C6) to derive

$$\pi N^{\rm AEA4'} = \int_0^{\mu} d\epsilon\, \Delta s^{(4)}(\epsilon) + \int_0^{\mu} d\epsilon\, n^{(2)}(\epsilon). \tag{C7}$$

The integral over $n^{(2)}$ is easy to evaluate numerically because $n^{(2)}(\epsilon)$ always equals an integer. To evaluate the integral over $n^{(2)}(\epsilon)$ we need the ϵ values where $n^{(2)}(\epsilon)$ jumps discontinuously between integer values. From the definition of the saw-tooth function $\langle x \rangle$ in the main text and Eq. (C5), we find that it jumps when

$$s^{(2)}(\epsilon_j) = j + \frac{1}{2}, \qquad j = 0, 1, 2, \cdots. \tag{C8}$$

This is just the second order eigenvalue expansion from Eq. (2) of the main text. More commonly this is called the second order WKB series quantization rule [37]. Inverting this equation numerically yields $\epsilon_j^{(2)}$, the second order WKB series approximation to ϵ_j. The other integral in Eq. (C7) is

$$\int_0^{\mu} d\epsilon\, \Delta s^{(4)}(\epsilon) = \frac{J''(\mu) - J''(0)}{5760}. \tag{C9}$$

To evaluate $J''(0)$ we carefully take the limit of $J''(\mu)$ as $\mu \to 0$ to derive

$$J''(0) = \frac{821 v^{(4)}(0)^2 - 344 v''(0) v^{(6)}(0)}{384 v''(0)^{5/2}}. \tag{C10}$$

We calculate $\mu^{\rm AEA4'}(N)$ by inverting $N^{\rm AEA4'}(\mu)$ numerically. The expression above diverges as $v''(0) \to 0$. This would happen for the pure quartic oscillator, $v(x) = x^4/2$. If it diverges we just set $J''(0)$ to 0.

The exact slab energy is completely specified by the 1D number staircase via Eq. (C6) and

$$E(\mu) = \mu N(\mu) - \int_0^{\mu} d\epsilon\, N(\epsilon). \tag{C11}$$

Plugging in $n^{(2)}$ ($n^{(2')}$) and collecting second order terms yields $E^{\rm AEA2(2')}(\mu)$. Plugging in $n^{(4')}$ yields

$$E^{\rm AEA4'}(\mu) = E^{\rm AEA2}(\mu) + \frac{\mu J''(\mu) - J'(\mu) + J'(0)}{5760\pi}, \tag{C12}$$

where

$$E^{\rm AEA2}(\mu) = \mu N^{\rm AEA2}(\mu) - \int_0^{\mu} d\epsilon\, N^{\rm AEA2}(\epsilon), \tag{C13}$$

where

$$N^{\rm AEA2}(\mu) = \int_0^\mu d\epsilon\, \frac{n^{(2)}(\epsilon)}{\pi}. \tag{C14}$$

To compute $E^{\rm AEA2}(\mu)$ numerically we only need the second order WKB series eigenvalues. In the limit $\mu \to 0$ we derive

$$J'(0) = \frac{9v^{(4)}(0)}{8\sqrt{v''(0)}}. \tag{C15}$$

If $v''(0) = 0$ we just set $J'(0)$ to 0. We set the particle number by plugging $\mu^{\rm AEA4'}(N)$ into $E^{\rm AEA4'}(\mu)$: $E^{\rm AEA4'}(N) = E^{\rm AEA4'}[\mu^{\rm AEA4'}(N)]$.

We approximated the AEA4' kinetic energy in Table I, of the main text, by subtracting away the AEA4' potential energy from the AEA4' total energy. The slab potential energy is related to the 1D potential energy via

$$V(\mu) = \int_0^\mu d\epsilon\, \frac{V_{\rm 1D}(\epsilon)}{\pi}. \tag{C16}$$

To evaluate $V^{\rm AEA4'}(\mu)$ numerically we plugged

$$V_{\rm 1D}^{\rm AEA4'}(\mu) = V^{\rm TF}[n^{(4')}(\mu)] + \Delta V^{(2)}[n^{(2')}(\mu)] + \Delta V^{(4)}[n^{(0')}(\mu)], \tag{C17}$$

into the integral above. $V^{\rm TF}(n)$, $\Delta V^{(2)}(n)$, and $\Delta V^{(4)}(n)$ are the lowest, second, and fourth order terms in the LS expansion of the 1D potential energy as a function of the exact 1D particle number, n. For the PT slab these terms are

$$V^{\rm TF}(n) = \sqrt{\frac{D}{2}}\frac{n^2}{2}, \qquad \Delta V^{(2)}(n) = -\frac{n^2}{32\sqrt{2D}},$$
$$\Delta V^{(4)}(n) = \frac{3n^2}{1024\sqrt{2D^3}}, \tag{C18}$$

Everywhere except Table I we approximated the AEA4' kinetic energy by subtracting the exact potential energy from the AEA4' total energy.

Appendix D: Differences between electron removal energies and chemical potentials

This section is devoted to showing how oscillating contributions can give rise to wildly differing accuracies of estimates for electron removal energies, depending on if the total energy curve or the chemical potential is used.

Figure S9 shows the exact and several approximate energy curves, each with the TF curve subtracted, as a function of N. The black curve (exact) is oscillating, as is the blue (AEA4') approximation. But the red curve (AEA2) contains no oscillations, as the oscillations cancel out of the total energy curve to 2nd order [which means that $E^{\rm AEA2}(\mu) = E^{\rm AEA2'}(\mu)$].

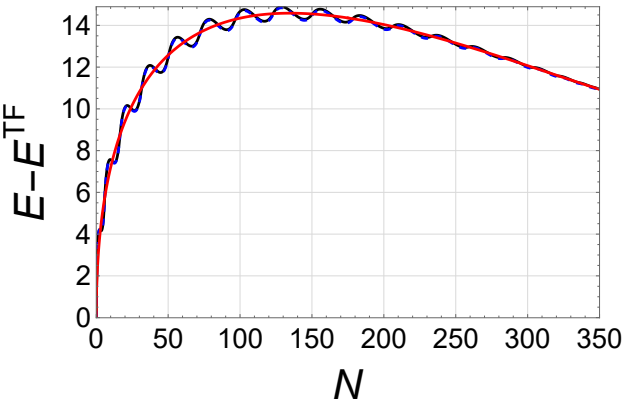

FIG. S9. The exact energy (black) and its AEA2 (red) and AEA4' (blue) approximations (with the TF energy subtracted), for the $M = 5$ PT slab in Table I of the main text.

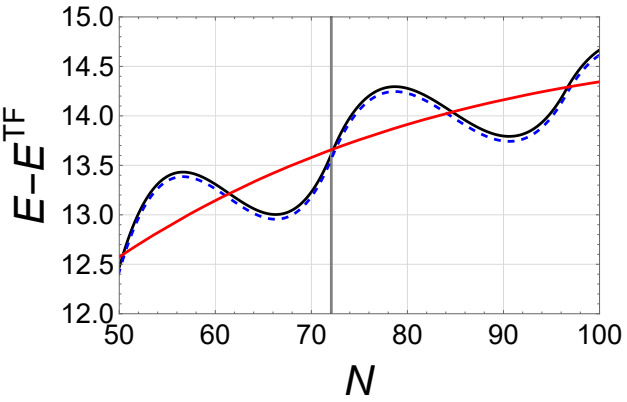

FIG. S10. A zoomed in view of Fig. S9. The gray line marks the occupation we examined in Table I of the main text.

Figure S10 simply zooms in on the energy curve in the region of the particle number corresponding to $\mu = D/2$, marked by the vertical line. Clearly the oscillations play a large role in the energy change if you remove 1/2 an electron when $\mu = D/2$. The red curve yields a very poor approximation to this energy difference. The exact energy satisfies $E'(N) = \mu$, but $dE^{\rm AEA2}/dN$ yields a poor approximation to the chemical potential. Instead we derive $\mu^{\rm AEA2}(N)$ by inverting $N^{\rm AEA2}(\mu)$. The blue AEA4' curve will clearly yield almost exact answers.

Table S1 contains many different approximations, for total energy differences and chemical potentials. Figure S11 shows the exact chemical potential and two approximations to it. The AEA2 chemical potential, calculated by inverting $N^{\rm AEA2}(\mu)$, captures the derivative discontinuities, while $dE^{\rm AEA2}/dN$, does not. This shows that relationships which hold exactly, for TF theory, and for GEA2, namely $E'(N) = \mu$, may fail at any given order when oscillatory terms are involved.

			Errors (mH)						
			IP			μ			
M	IP	μ	TF	AEA2	AEA4'	TF	AEA2'	AEA2	AEA4'
1	5.557	6.342	−63	−3	0.0622	−242	−41	0.010	−0.0532
2	17.607	18.000	−172	−131	0.0168	−239	−21	0.013	−0.0126
3	35.224	35.486	−204	−166	0.0061	−238	−14	0.009	−0.0048
4	58.603	58.799	−217	−180	0.0028	−237	−11	0.006	−0.0023
5	87.784	87.941	−224	−187	0.0015	−237	−9	0.004	−0.0013
6	122.781	122.912	−227	−191	0.0009	−237	−7	0.003	−0.0008
7	163.599	163.711	−230	−194	0.0006	−237	−6	0.003	−0.0005
8	210.240	210.339	−231	−196	0.0004	−237	−5	0.002	−0.0004
9	262.707	262.794	−232	−197	0.0003	−237	−5	0.002	−0.0003
10	321.000	321.079	−233	−198	0.0002	−237	−4	0.001	−0.0002

TABLE S1. Same as Table II of the main text but with the AEA2' and AEA4' approximations.

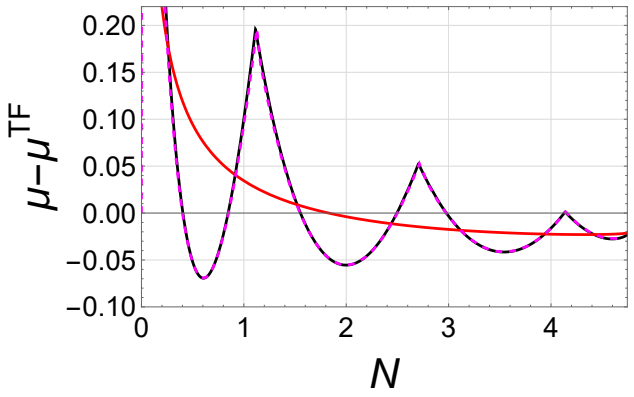

FIG. S11. The exact chemical potential for a PT slab with $D = 10$ (black), dE^{AEA2}/dN (red), and $\mu^{\mathrm{AEA2}}(N)$ (magenta). We have subtracted the TF chemical potential from all curves.

Appendix E: Breakdown of the AEA4' approximation in our bond stretching table

Figure S12 plots several of the errors listed in Table III of the main text as functions of the separation between the PT centers.

Appendix F: Tables of energies for PT slabs and PT dimers

This section contains tables that supplement those in the main text.

Table S2 shows the total energies (not just the kinetic energies) of the calculations in Table I of the main text. In this case, any functionals evaluated on the exact density include the exact potential energy by construction. Just as in the self-consistent TF calculation, we expect errors on (some version of) self-consistent densities to be larger.

Tables S3-S5 supplement Table III of the main text, showing total kinetic energies of the PT dimer slabs, not just binding energies, so that approximations cannot benefit from cancellation of errors between the PT dimer slab and the separated 'atomic' slabs. We also give the corresponding total energy and binding energy.

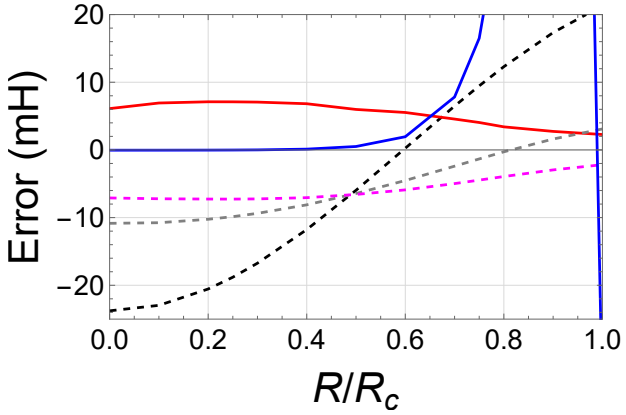

FIG. S12. The errors in Table III of the main text. Legend: TF (black), GEA2 (gray), MGE2 (magenta), AEA2 (red), AEA4' (blue). Functionals acting on the exact density are denoted with dashed lines.

Table S6 shows the 1D ground state WKB eigenvalues and their leading corrections for the PT dimer as a function of well-separation. By $R = 0.8R_c$, the leading correction has a larger error than WKB itself, signaling the incipient failure of the asymptotic series.

				Errors (mH)						
				Potential Functionals			Density Functionals			
M	D	N	E/N	TF	AEA2	AEA4'	TF	GEA2	MGE2	GEA4
1	12.685	1.293	4.312	−192	9.2	0.02522	−156	−41	−8	−2
2	36.000	6.525	12.189	−190	3.1	0.00298	−159	−35	1	−6
3	70.971	18.318	24.005	−189	1.6	0.00076	−162	−31	7	−7
4	117.599	39.293	39.759	−189	0.9	0.00027	−164	−28	11	−6
5	175.883	72.075	59.451	−189	0.6	0.00012	−165	−26	14	−6
6	245.824	119.288	83.082	−189	0.4	0.00006	−166	−25	16	−6
7	327.422	183.555	110.651	−189	0.3	0.00004	−167	−24	18	−6
8	420.677	267.500	142.159	−189	0.3	0.00002	−168	−23	19	−6
9	525.589	373.746	177.605	−189	0.2	0.00001	−168	−22	21	−5
10	642.157	504.918	216.990	−189	0.2	0.00001	−169	−21	22	−5

TABLE S2. Same as Table I of the main text, but for the total energy.

		Errors (mH)									
		Potential Functionals					Exact Density or μ				
R/R_c	T	TF	GEA2	AEA2'	AEA2	AEA4'	TF	GEA2	MGE2	GEA4	AEA4'(μ)
0	1.890	34	−19	11.84	3.1	0.02	−77	−22	−5.5	−12	0.20
0.1	1.881	36	−16	12.51	3.9	0.02	−76	−21	−5.6	−12	0.20
0.2	1.858	39	−12	12.24	4.1	0.04	−74	−21	−5.6	−12	0.19
0.25	1.840	40	−9	11.90	4.1	0.05	−72	−21	−5.6	−12	0.19
0.3	1.820	42	−6	11.48	4.0	0.07	−70	−20	−5.6	−12	0.18
0.4	1.770	46	1	10.31	3.8	0.18	−65	−19	−5.4	−11	0.18
0.5	1.711	49	8	8.39	2.9	0.57	−59	−17	−5.0	−10	0.21
0.6	1.644	50	14	6.74	2.5	2.01	−53	−15	−4.3	−9	0.35
0.7	1.575	50	17	4.49	1.5	7.89	−47	−13	−3.4	−7	0.71
0.75	1.539	49	18	3.32	1.0	16.56	−44	−12	−2.8	−7	1.00
0.8	1.504	47	17	2.00	0.4	37.29	−41	−11	−2.3	−6	1.38
0.9	1.435	43	16	−0.02	−0.3	315.89	−36	−9	−1.3	−4	2.43
1	1.369	37	12	−1.79	−0.8	−37.27	−32	−8	−0.6	−3	−0.26

TABLE S3. Same as Table III of the main text, but showing the total kinetic energies, not the kinetic binding energies.

		Errors (mH)							
		Potential Functionals			Exact Density or μ				
R/R_c	$E-2E_A$	TF	AEA2	AEA4'	TF	GEA2	MGE2	GEA4	AEA4'(μ)
0	1.174	−39	−9.2	−0.04	−23.8	−10.8	−7.1	−12	−0.23
0.1	1.162	−39	−9.4	−0.04	−23.0	−10.8	−7.2	−12	−0.24
0.2	1.127	−36	−9.7	−0.03	−20.5	−10.2	−7.3	−12	−0.24
0.25	1.100	−34	−9.9	−0.02	−18.8	−9.9	−7.3	−12	−0.25
0.3	1.068	−32	−10.0	0.01	−16.7	−9.4	−7.2	−12	−0.25
0.4	0.988	−27	−10.1	0.12	−11.8	−8.1	−7.1	−12	−0.25
0.5	0.887	−21	−9.7	0.51	−6.0	−6.4	−6.6	−11	−0.22
0.6	0.767	−13	−8.7	1.95	0.3	−4.5	−5.9	−9	−0.08
0.7	0.630	−6	−7.2	7.82	6.5	−2.4	−5.0	−8	0.27
0.75	0.556	−2	−6.3	16.49	9.5	−1.3	−4.5	−7	0.57
0.8	0.479	2	−5.3	37.23	12.3	−0.3	−3.9	−6	0.95
0.9	0.315	9	−3.4	315.82	17.3	1.6	−3.0	−4	2.00
1	0.143	15	−1.7	−37.33	21.3	3.1	−2.2	−3	−0.69

TABLE S4. Same as Table III of the main text, but with the total binding energy.

		Errors (mH)							
		Potential Functionals			Exact Density or μ				
R/R_c	E	TF	AEA2	AEA4'	TF	GEA2	MGE2	GEA4	AEA4'(μ)
0	2.845	−99	−7.0	0.02	−77	−22	−5.48	−12	0.20
0.1	2.833	−98	−7.1	0.02	−76	−21	−5.60	−12	0.20
0.2	2.798	−95	−7.4	0.04	−74	−21	−5.64	−12	0.19
0.25	2.772	−94	−7.6	0.05	−72	−21	−5.65	−12	0.19
0.3	2.740	−92	−7.7	0.07	−70	−20	−5.62	−12	0.18
0.4	2.659	−86	−7.8	0.18	−65	−19	−5.44	−11	0.18
0.5	2.558	−80	−7.4	0.57	−59	−17	−4.96	−10	0.21
0.6	2.438	−73	−6.5	2.01	−53	−15	−4.29	−9	0.35
0.7	2.301	−65	−5.0	7.89	−47	−13	−3.36	−7	0.71
0.75	2.227	−61	−4.0	16.56	−44	−12	−2.84	−7	1.00
0.8	2.150	−57	−3.1	37.29	−41	−11	−2.31	−6	1.38
0.9	1.986	−51	−1.2	315.89	−36	−9	−1.33	−4	2.43
1	1.814	−45	0.5	−37.27	−32	−8	−0.56	−3	−0.26

TABLE S5. Same as Table III of the main text, but with the total energy relative to the bottom of the well. The dimer well depth is $\mathcal{D} = 6\ \mathrm{sech}^2(R/2)$.

		Errors	
R/R_c	ϵ_0	WKB0	WKB2
0	1.500	0.107	−0.00056
0.1	1.489	0.106	−0.00061
0.2	1.456	0.101	−0.00078
0.25	1.431	0.097	−0.00094
0.3	1.402	0.093	−0.00116
0.4	1.329	0.083	−0.00194
0.5	1.239	0.069	−0.00347
0.6	1.134	0.053	−0.00640
0.7	1.016	0.034	−0.01186
0.75	0.954	0.024	−0.01604
0.8	0.890	0.013	−0.02153
0.9	0.756	−0.011	−0.03734
1	0.618	−0.036	−0.06000
∞	2.000	0.199	−0.00208

TABLE S6. The exact ground state eigenvalues (relative to the bottom of the well) and their zeroth and second order WKB approximations for the PT dimers in Table III of the main text. The last row, $R/R_c = \infty$, corresponds to 2, $D = 3$, PT slabs infinity far apart (so all of the quantities are double those of a single PT slab).